Importin 8 mediates m^7G cap-sensitive nuclear import of the eukaryotic translation initiation factor eIF4E

Laurent Volpon[a,1], Biljana Culjkovic-Kraljacic[a,1], Michael J. Osborne[a,1], Anup Ramteke[a], Qingxiang Sun[b], Ashley Niesman[b], Yuh Min Chook[b], and Katherine L. B. Borden[a,2]

[a]Institute of Research in Immunology and Cancer, Department of Pathology and Cell Biology, Université de Montréal, Montreal, QC, H3T 1J4, Canada; and [b]Department of Pharmacology, University of Texas Southwestern Medical Center at Dallas, Dallas, TX 75390-9041

Edited by Joan A. Steitz, Howard Hughes Medical Institute, New Haven, CT, and approved March 17, 2016 (received for review December 10, 2015)

Regulation of nuclear-cytoplasmic trafficking of oncoproteins is critical for growth homeostasis. Dysregulated trafficking contributes to malignancy, whereas understanding the process can reveal unique therapeutic opportunities. Here, we focus on eukaryotic translation initiation factor 4E (eIF4E), a prooncogenic protein highly elevated in many cancers, including acute myeloid leukemia (AML). Typically, eIF4E is localized to both the nucleus and cytoplasm, where it acts in export and translation of specific methyl 7-guanosine (m^7G)–capped mRNAs, respectively. Nuclear accumulation of eIF4E in patients who have AML is correlated with increased eIF4E-dependent export of transcripts encoding oncoproteins. The subcellular localization of eIF4E closely correlates with patients' responses. During clinical responses to the m^7G-cap competitor ribavirin, eIF4E is mainly cytoplasmic. At relapse, eIF4E reaccumulates in the nucleus, leading to elevated eIF4E-dependent mRNA export. We have identified importin 8 as a factor that directly imports eIF4E into the nucleus. We found that importin 8 is highly elevated in untreated patients with AML, leading to eIF4E nuclear accumulation. Importin 8 only imports cap-free eIF4E. Cap-dependent changes to the structure of eIF4E underpin this selectivity. Indeed, m^7G cap analogs or ribavirin prevents nuclear entry of eIF4E, which mirrors the trafficking phenotypes observed in patients with AML. Our studies also suggest that nuclear entry is important for the prooncogenic activity of eIF4E, at least in this context. These findings position nuclear trafficking of eIF4E as a critical step in its regulation and position the importin 8–eIF4E complex as a novel therapeutic target.

eIF4E | importin 8 | nuclear import | m^7G cap

Control of nuclear trafficking is critical for regulation of proliferation and survival. Here, we reveal a mechanism for the trafficking of the eukaryotic translation initiation factor 4E (eIF4E), which is elevated in an estimated 30% of cancers (1). In mice, eIF4E overexpression alone is sufficient to drive development of a variety of cancers (2). eIF4E acts in the nuclear export and translation of specific mRNAs (3, 4). In fact, eIF4E enhances the export of over 3,500 mRNAs, many of which encode oncoproteins (3, 5–7). In this way, eIF4E modulates gene expression through increasing cytoplasmic levels of transcripts via enhanced export and, in some cases, increasing the number of ribosomes associated with these transcripts in the cytoplasm. Although different elements in the target transcripts are required for the mRNA export or translation function of eIF4E, both require the methyl 7-guanosine (m^7G) cap on the 5′ end of the mRNA. Several lines of evidence indicate that the mRNA export activity of eIF4E contributes to its oncogenic potential (5–8). Thus, understanding the mechanisms that underlie its nuclear-cytoplasmic trafficking is important.

eIF4E is not only elevated but also accumulates in the nucleus of some cancers, including subsets of acute myeloid leukemia (AML) and some lymphomas (8–10). AML is a highly aggressive malignancy with poor overall survival (11–13). For these cancer subtypes, the vast majority of eIF4E is found in the nucleus, correlating with highly elevated eIF4E-dependent mRNA export (9, 10, 14). Accordingly, eIF4E activity was targeted in two AML clinical trials using ribavirin, which acts as a cap competitor (9, 14). In these trials, ribavirin treatment impaired eIF4E activity in patients who had AML, which correlated with clinical responses, including some remissions. In vitro, eIF4E binds ribavirin under physiological solution conditions (15–18). In cell culture, ribavirin inhibits eIF4E activity, as observed by several groups (19–21). Indeed, cell growth is no longer inhibited by ribavirin in cells pretreated with RNAi to eIF4E (21).

eIF4E localization is altered by treatment with m^7G cap analogs or ribavirin. Specifically, m^7G cap and ribavirin lead to cytoplasmic enrichment and nuclear depletion of eIF4E in treated cell lines and patients (15, 22, 23). In patients, eIF4E relocalization to the cytoplasm correlates with clinical responses (9, 14). At relapse, eIF4E redistributes to the nucleus, correlating with a loss of the eIF4E–ribavirin interaction due to either ribavirin glucuronidation or impaired cellular uptake of ribavirin (14, 18). These clinical observations highlight the importance of identifying the molecular mechanisms that underpin eIF4E nuclear trafficking. However, there is no molecular understanding of this process. For instance, eIF4E lacks a classical nuclear localization signal (c-NLS) or a proline-tyrosine (PY)-NLS (24). Here, we identify importin 8 as a direct mediator of eIF4E nuclear import. Further, eIF4E nuclear entry is regulated by a competition between m^7G cap and importin 8 binding. Our findings provide insights into the control of eIF4E activity through modulation of its subcellular localization.

Significance

Dysregulated nuclear trafficking of oncoproteins contributes to cancer. Here, we study the trafficking of eukaryotic translation initiation factor 4E (eIF4E) in acute myeloid leukemia (AML), where eIF4E is highly elevated and accumulates in the nucleus. Nuclear eIF4E promotes export of networks of transcripts encoding oncoproteins. During clinical responses to eIF4E-targeted therapy in patients who have AML, the distribution of eIF4E becomes almost entirely cytoplasmic. At relapse, eIF4E is again mainly nuclear. Our studies provide a molecular understanding for eIF4E trafficking, through association with importin 8. We provide a molecular basis for importin 8 selectivity for certain forms of eIF4E and demonstrate the relevance of its nuclear localization to its oncogenic potential, thereby positioning the importin 8–eIF4E interaction as a novel therapeutic target.

Author contributions: L.V., B.C.-K., M.J.O., Q.S., A.N., Y.M.C., and K.L.B.B. designed research; L.V., B.C.-K., M.J.O., A.R., Q.S., and A.N. performed research; L.V., B.C.-K., M.J.O., and Y.M.C. contributed new reagents/analytic tools; L.V., B.C.-K., M.J.O., Q.S., A.N., Y.M.C., and K.L.B.B. analyzed data; and L.V., B.C.-K., M.J.O., Y.M.C., and K.L.B.B. wrote the paper.

Conflict of interest statement: The authors declare no conflict of interest.

This article is a PNAS Direct Submission.

Freely available online through the PNAS open access option.

[1]L.V., B.C.-K., and M.J.O. contributed equally to this work.

[2]To whom correspondence should be addressed. Email: katherine.borden@umontreal.ca.

This article contains supporting information online at www.pnas.org/lookup/suppl/doi:10.1073/pnas.1524291113/-/DCSupplemental.

Results

eIF4E Is an Importin 8 Cargo. To elucidate mechanisms for its nuclear entry, we examined the ability of GST-eIF4E to bind a panel of import karyopherins (importins), including importins 4, 5, 7, 8, and 9; importin-α; and Kapβ2. All of these bacterially produced and purified importins are active because they all bind a form of yeast Ran•GTP (guanosine triphosphate) [Glutathione S-transferase (GST)-GSP1] with mutations and deletions (GST-GSP1 1–179, Q71L) that stabilize the GTP-bound state (25) (Fig. S1*A*). Of the importins tested, only importin 8 bound eIF4E (Fig. 1*A* and Fig. S1*B*). We observed that excess human wild-type Ran•GTP released importin 8 from its eIF4E cargo (Fig. 1*A*) a feature common to importin–cargo interactions (26). Thus, eIF4E is a potential cargo for importin 8.

We carried out in vitro nuclear import assays (27) to establish whether the importin 8–eIF4E interaction was functional (Fig. 1*B* and Fig. S1 *C–E*). Import of GST-eIF4E was monitored in permeabilized U2OS cells using immunofluorescence in conjunction with confocal laser microscopy. Nuclear import of eIF4E was quantified using standard procedures (Fig. S1*E*). We used a GST antibody to detect exogenous eIF4E specifically. Import assays were performed using a buffer with a mixture of cofactors required for karyopherin-dependent nuclear import (*Materials and Methods*). In the presence of this buffer, GST-eIF4E remained in the cytoplasm, whereas addition of importin 8 led to its nuclear entry (Fig. 1*B* and Fig. S1*E*). GST-GSP1 addition impaired importin 8-mediated entry of eIF4E (Fig. 1*B* and Fig. S1*E*). Similarly, eIF4E did not enter the nucleus in the absence of wild-type human Ran (Fig. S1 *D* and *E*). Thus, importin 8 imports eIF4E into the nucleus in vitro in a Ran-dependent fashion.

Consistent with our above GST pull-down assays, addition of purified importins that did not bind eIF4E-GST (e.g., importins 4, 5, 9) did not import eIF4E into the nucleus (Fig. 1*B* and Fig. S1 *D* and *E*). Further, we tested if another member of the eIF4E family, eIF4E3, was also a cargo. eIF4E3 was examined because it has a similar overall fold to eIF4E but a different charge distribution (28). Importantly, eIF4E3 was neither imported by nor bound to importin 8 (Fig. S2). Thus, the effects of importin 8 are not generalizable to the eIF4E family, and, similarly, not all importins import eIF4E.

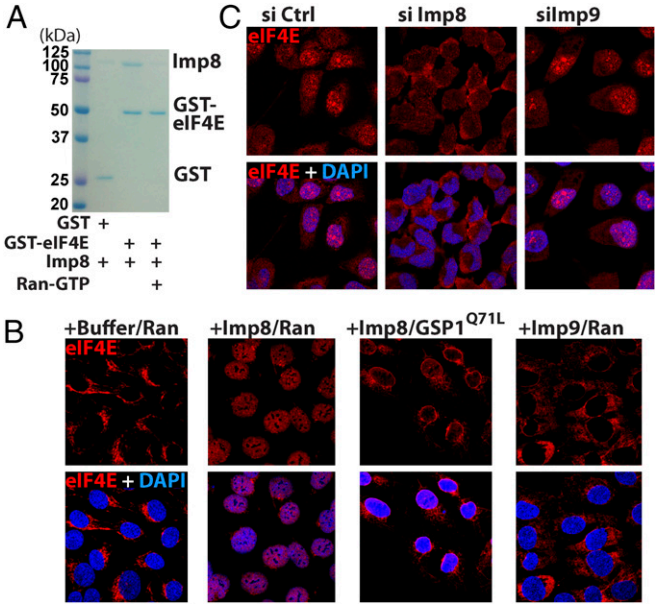

Fig. 1. eIF4E is an importin 8 cargo. (*A*) GST pull-down assay for importin 8 and eIF4E-GST visualized by Coomassie Blue staining. (*B*) In vitro nuclear import assays using purified GST-eIF4E in digitonin-permeabilized U2OS cells as shown. Additional experiments and quantitations are shown in Fig. S1 *D* and *E*. (*C*) Confocal micrographs monitoring endogenous eIF4E localization as a function of importin 8 knockdown (si Imp8) and importin 9 knockdown (si Imp9) versus control (si Ctrl). Western blots confirm knockdown with no effect on eIF4E levels in Figs. S1*C* and S3*H*. Each confocal micrograph is a single section through the plane of the cell with a magnification of 63× and no digital zoom.

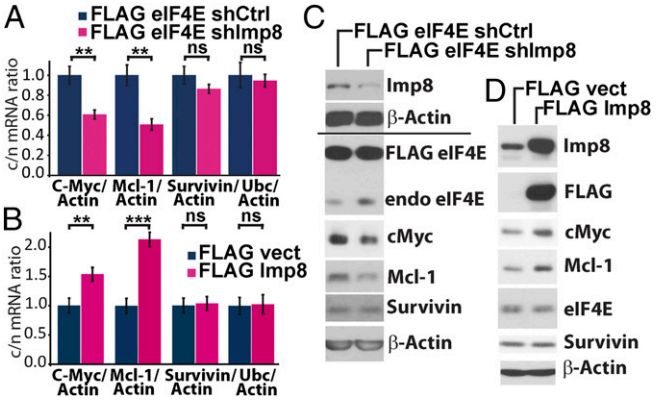

Fig. 2. eIF4E nuclear trafficking affects its mRNA export activity. Effects of importin 8 (Imp8) knockdown on target mRNA export (*A*) and protein levels (*C*) in eIF4E-overexpressing (FLAG eIF4E) cells. Short hairpin control (shCtrl) indicates RNAi control, and c/n indicates the cytoplasmic-to-nuclear ratio. The c/n of tested mRNAs is shown. Results for endogenous eIF4E (endo eIF4E) upon importin 8 knockdown are shown in Fig. S3 *A* and *B*. Effects of importin 8 overexpression in the presence of endogenous eIF4E at the mRNA export (*B*) and protein levels (*D*) relative to vector controls (FLAG vect). Total mRNAs levels are unchanged (Fig. S3*D*), and fractionation controls are shown in Fig. S3*C*. Data are the mean ± SD. $^{**}P < 0.01$; $^{***}P < 0.001$. ns, not significant.

Next, we assessed the role of importin 8 in eIF4E import in U2OS cells. Note that in intact cells, eIF4E forms nuclear bodies as well as being present in the nucleoplasm and cytoplasm (5, 7, 23). Levels of nuclear eIF4E are unchanged in importin 9 knockdown cells relative to controls (Fig. 1*C* and Fig. S1*C*). However, importin 8 knockdown reduced nuclear levels by threefold without altering eIF4E protein levels (Fig. 1*C* and Fig. S1*C*). The knockdowns of importin 8 and importin 9 were validated by Western blot (Fig. S1*C*). In summary, importin 8 mediates eIF4E nuclear entry in vitro and in intact cells.

Importin 8 Affects eIF4E-Dependent mRNA Export. We examined whether modulating nuclear entry of eIF4E has an impact on its mRNA export activity. To assess this effect, cells were fractionated into nuclear and cytoplasmic components and mRNA levels in each fraction were examined using quantitative PCR (qPCR) (Fig. 2*A*). Fractionation quality was assessed using U6snRNA and $tRNA^{lys}$ for nuclear and cytoplasmic fractions, respectively (Fig. S3*C*, *Top*). Importantly, importin 8 knockdown, and thus cytoplasmic retention of eIF4E, led to nuclear accumulation of endogenous eIF4E mRNA export targets, such as c-Myc and Mcl-1, without altering their total mRNA levels (Fig. 2*A* and Fig. S3*D*, *Top*). Concomitantly, c-Myc and Mcl-1 protein levels were reduced, consistent with their lowered mRNA export (Fig. 2*C*). Importin 8 knockdown did not affect eIF4E protein levels or mRNA export of negative controls, such as survivin and β-actin. As a specificity control, we examined the effects of importin 9 knockdown (Fig. S3 *E–H*). In contrast to importin 8, importin 9 knockdown did not impair eIF4E-dependent mRNA export or reduce protein levels of eIF4E targets. Interestingly, importin 9 knockdown led to cell death, where we postulate increased Mcl-1 levels were a compensatory mechanism unrelated to mRNA export. Thus, reduction in importin 8 specifically impairs eIF4E-dependent mRNA export through inhibition of eIF4E nuclear entry.

Conversely, importin 8 overexpression stimulated eIF4E-dependent mRNA export of Mcl-1 and c-Myc mRNAs, but not negative controls (e.g., survivin, ubiquitin) (Fig. 2 *B* and Fig. S3*D*, *Bottom*). This increased export corresponded to elevated

c-Myc and Mcl-1 protein levels. In contrast, importin 9 overexpression did not alter the levels of eIF4E targets (Fig. S3*J*). Consistently, importin 8 overexpression led to increased levels of nuclear eIF4E (Fig. S3*K*). Thus, importin 8 promotes eIF4E-dependent mRNA export activity by promoting its reentry into the nucleus, a prerequisite for its export activity.

The Transformation Activity of eIF4E Is Related to Its Nuclear Localization. Given the close ties between eIF4E-dependent mRNA export and its oncogenic potential (6, 7), we monitored the relevance of increased nuclear eIF4E trafficking to this activity (Fig. 3*A*). We measured loss of contact inhibition using an anchorage-dependent foci formation assay as a function of modulating eIF4E localization using either U2OS cells or immortalized, but not transformed, fibroblasts (Fig. 3 and Fig. S4 *A–E*). First, we found that in eIF4E-overexpressing cells, importin 8 knockdown reduces foci number by about fivefold relative to RNAi controls in U2OS cells and approximately threefold effects in mouse embryonic fibroblasts (Fig. 3*A* and Fig. S4*D*). Western blots confirm importin 8 knockdown and no change to eIF4E levels (Fig. 2*C*). These observations suggest that lower levels of nuclear eIF4E reduced its prooncogenic activity. Conversely, importin 8 overexpression led to an over threefold increase of foci number relative to vector in U2OS cells and to an approximately fourfold increase in fibroblasts (Fig. 3*B* and Fig. S4*E*). Further, RNAi knockdown of eIF4E in importin 8-overexpressing cells completely impaired the foci formation activity of importin 8 (Fig. 3*B*). Importantly, eIF4E knockdown did not alter the levels of the importin 8-FLAG construct (Fig. S4*A*). Finally, importin 9 overexpression did not modulate the number of foci relative to vector (Fig. S4 *B*, *C*, and *E*); thus, this transformation activity is not universal for all importins. We also examined the relevance of nuclear entry to the invasion activity of eIF4E in Matrigel assays (Fig. S4*F*). Importin 8 knockdown reduced eIF4E-mediated invasion by approximately threefold relative to RNAi controls in U2OS cells. Taken together, these findings suggest that its nuclear localization increased the foci formation and invasion activities of eIF4E.

Effects of Adding an NLS to eIF4E. Given these findings, we assessed the effects of the addition of a c-NLS to eIF4E (29). The eIF4E+NLS protein is more nuclear than wild-type protein but still retains substantial cytoplasmic localization, suggesting it is associated with a strong nuclear export signal, as we observed previously (Fig. S5*A*). This observation also suggests that eIF4E+NLS still transits between compartments but likely with a reduced cytoplasmic dwell time due to faster cycling into the nucleus. Overexpression of eIF4E+NLS led to increased eIF4E-dependent mRNA export as well as increased levels of the corresponding proteins relative to wild-type eIF4E or vector controls (Fig. S5 *B* and *C*). Further, eIF4E+NLS expression yielded over twofold more foci than wild-type eIF4E and over 13-fold more than vector controls (Fig. S5*D*). We note that eIF4E+NLS levels were consistently lower than levels for wild-type protein, likely leading to an underestimation of its effects on mRNA export and transformation. Together, these studies suggest that increased nuclear trafficking of eIF4E via an NLS or by importin 8 overexpression increases its oncogenic potential.

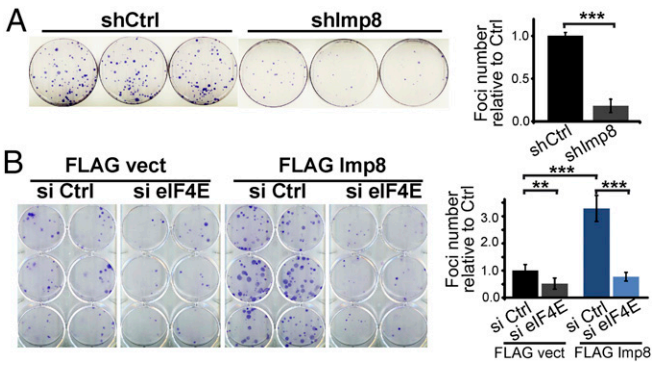

Fig. 3. Importin 8 transformation activity is eIF4E-dependent. Foci assays in U2OS cells as a function of importin 8 shRNA knockdown (*A*, shImp8) or importin 8 overexpression (*B*, FLAG Imp8). shCtrl and FLAG vect indicate corresponding controls. (*Right*) Foci numbers relative to controls are quantified. Data are the mean ± SD. $^{**}P < 0.01$; $^{***}P < 0.001$. Western blots for FLAG Imp8 and eIF4E expression are shown in Fig. S4*A*.

Molecular Basis of the Importin 8–eIF4E Interaction. We used NMR methods to determine the molecular basis for the importin 8–eIF4E interaction. We monitored the ^{1}H-^{15}N HSQC (heteronuclear single quantum coherence) spectra of ^{15}N-labeled eIF4E as a function of importin 8 addition. We observed extensive signal broadening for eIF4E resonances (Fig. 4*A* and Fig. S6 *A* and *B*), which occurred because of the slower tumbling of the eIF4E–importin 8 complex (145 kDa) compared with eIF4E (25 kDa). Residues in the structured region of eIF4E (26–217) were affected even at low molar ratios of importin 8 to eIF4E (e.g., at 0.03125:1), consistent with an estimated off-rate of ~100 s^{-1} and a K_d in the low micromolar range (assuming diffusion limited on-rates). In contrast, the flexible N terminus of eIF4E is visible even at twofold excess importin 8, indicating that this region is not involved in binding (Fig. S6*B*).

Our HSQC analysis indicated that regions in and around the cap-binding site were likely directly involved in the importin 8 interaction (Fig. 4*C*). The m^7G cap-binding site can be roughly divided into two regions: (*i*) residues W56 and W102, which bind the m^7G moiety of the cap (1, 30), and (*ii*) residues R157, K159, and K162, which form a positively charged patch to bind the phosphate moieties of the cap (1, 31) (Fig. 4*D* and Fig. S7*A*). Analysis of intensity changes of eIF4E upon importin 8 addition revealed that the most affected residues were generally located around this positively charged patch, with minor affects distributed throughout the structure (Fig. 4*C*).

Given that our NMR data pointed to the cap-binding site as a key part of the interaction surface of eIF4E, we assessed whether importin 8 also associated with cap-bound forms of eIF4E. Note that our above GST pull-down and NMR experiments used apo-eIF4E. Strikingly, we observed that addition of a m^7G cap analog (m^7GDP) to a preformed complex of ^{15}N-labeled eIF4E and unlabeled importin 8 led to reappearance of resonances in the HSQC for eIF4E, but now in cap-bound positions (Fig. 4 *A* vs. *B* and Figs. S6*C* and S8). Thus, addition of the m^7G cap analog substantially reduced the affinity of eIF4E for importin 8. We confirmed this observation using a GST pull-down assay, where the eIF4E–importin 8 complex dissembled upon addition of excess m^7GDP (Fig. 4*E*). We also found that addition of m^7G-capped mRNA, which better reflects the in vivo ligand, reduced importin 8 binding to eIF4E (Fig. 4*F*). Thus, excess m^7G-capped RNA or m^7G cap analog prevents direct binding of eIF4E to importin 8.

These findings led us to investigate whether cap binding altered the nuclear import of eIF4E. Indeed, the presence of excess m^7G cap analog severely impaired eIF4E nuclear entry by over 50-fold (Fig. 4*H* and Fig. S1*F*), presumably by disrupting the eIF4E–importin 8 complex, consistent with our NMR and pull-down studies. Importantly, m^7G cap addition did not impair entry of the eIF4E W56A cap-binding mutant (Fig. 4*H* and Fig. S1*F*) as expected, given the 50-fold reduction in affinity of this mutant for the m^7G cap (6). Next, we examined the effects of m^7G cap addition on an importin α/β cargo by monitoring trafficking of the GST-NLS-GFP cargo (31). Import assays carried out in the presence or absence of m^7G cap showed no difference in GST-NLS-GFP distribution, with GST-NLS-GFP located primarily in the nucleus (Fig. 4*G* and Fig. S1*G*). From the above studies, we conclude that importin 8 only imports apo-eIF4E. Further, m^7G cap specifically impairs import of eIF4E, but not of cargoes using other import pathways.

Inspection of the charge distribution on apo- and cap-bound eIF4E structures reveals that the large positively charged patch in apo-eIF4E centered around residues R157, K159, and K162 is

BIOCHEMISTRY

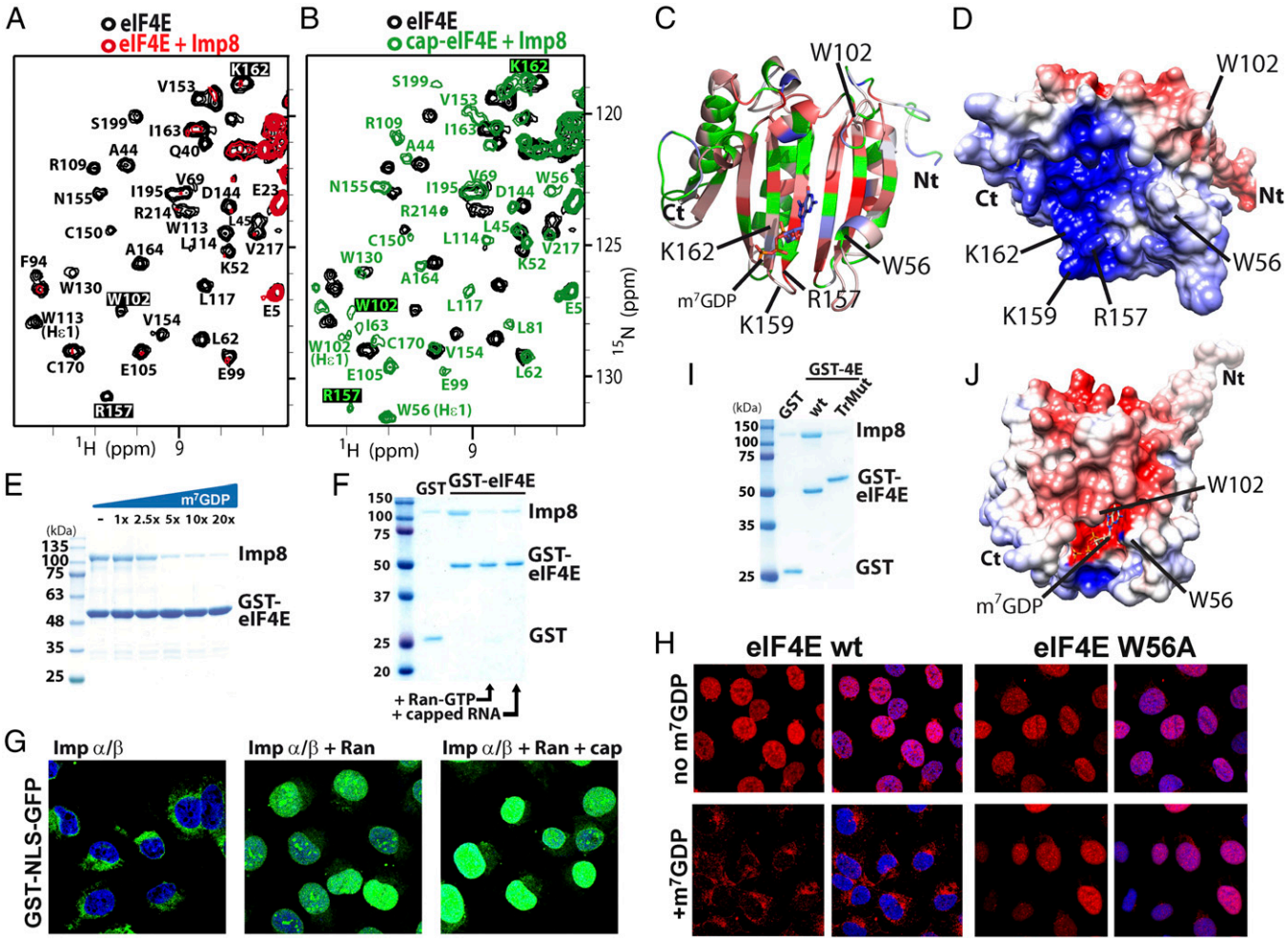

Fig. 4. Importin 8 binding to eIF4E is sensitive to m^{7}G cap addition. ^{1}H-^{15}N HSQC spectra of eIF4E (black) upon addition of twofold molar excess unlabeled importin 8 (*A*, red), or subsequent addition of 20-fold molar excess m^{7}GDP cap (*B*, green). Assignments are shown for the backbone H^N and the Trp indoles Hε1. The full HSQC spectra are shown in Fig. S6. (*C*) Changes in cross-peak intensities are mapped onto the apo-eIF4E structure [Protein Data Bank (PDB) ID code 2GPQ] (30). Residues are color-coded according to intensity changes of the cross-peaks based on a color ramp ranging from blue (no change), to white (medium change), to red (largest change) at a molar ratio for eIF4E/importin 8 of 1:0.25. Overlapping or unassigned residues are green. Key cap-binding residues are shown, and the m^{7}GDP cap is depicted with lines, according to the cap-bound eIF4E structure (PDB ID code 3AM7). For clarity, only the structured region is shown, residues 26–217. (*D*) Electrostatic surface representation of apo-eIF4E (same orientation as in *C*). Acidic (negatively charged) and basic (positively charged) regions are in red and blue, respectively. Effect of increasing concentration of the m^{7}GDP cap (one- to 20-fold) (*E*) and twofold molar excess m^{7}G-capped RNA (*F*) on the association of importin 8 to GST-eIF4E by GST pull-down assay. (*G*) Import assay with GST-NLS-GFP in the presence of importin α/β2, Ran, or 50 μM m^{7}G cap as indicated. DAPI is in blue. (*H*) In vitro nuclear import assays for eIF4E wild type (*Left*) and cap-binding mutant W56A (*Right*) ± 50 μM m^{7}GDP cap analog (eIF4E in red and DAPI in blue). (*I*) GST pull-down assay with eIF4E-GST or eIF4E-TrMut-GST. (*J*) Surface charge distribution within the cap-binding pocket of m^{7}GDP-bound eIF4E (PDB ID code 3AM7). Key residues and the m^{7}GDP cap are shown. (Magnification: *G* and *H*, 63× with no additional zoom.) Quantitations for confocal images are shown in Fig. S1 *F* and *G*.

no longer present in the cap-bound form (Fig. 4 *D* and *J*). This change occurs because m^{7}G cap binding leads to closure of the W56 and W102 loops with concomitant reduction of the positive charge due to the presence of the cap analog phosphates (30). Consistently, our NMR data indicated that residues at this positively charged surface were significantly perturbed even at low molar importin 8/eIF4E ratios (Fig. 4*C*). To examine the relevance of this surface for importin 8 binding, we generated a triple mutant (TrMut) whereby R157, K159, and K162 were mutated to glutamates to imbue this surface with a negative charge (Fig. S9 *A* and *B*). NMR and CD studies indicated the TrMut was folded (Fig. S9 *C* and *D*). GST pull-down experiments showed that the TrMut had a marked reduction in affinity for importin 8 relative to wild-type eIF4E (Fig. 4*I*). Thus, mutation of the positive surface in the cap-binding site substantially reduces the affinity of eIF4E for importin 8. We note that mutation of W56 did not alter binding to importin 8 or nuclear trafficking of eIF4E (Fig. 4*H*, *Right* and Figs. S1*F* and S7 *B–D*). These observations indicate that the positive patch within the cap-binding site is specifically required for importin 8 trafficking, and not the cap-binding site as a whole.

Mutation of the positive patch suggested that the interaction of eIF4E with importin 8 was electrostatically based. Thus, we examined the salt sensitivity of the interaction using NMR and pull-down assays with wild-type proteins (Fig. S9 *E* and *F*). As expected, increasing NaCl from 100 to 500 mM impaired complex formation. Taken together with the TrMut, these studies strongly suggest that a negative patch on importin 8 interacts with the positive patch in the vacant cap-binding site. However, our HSQC data also indicate that residues throughout the eIF4E structure were perturbed by importin 8, suggesting that importin 8 contacts additional surfaces on eIF4E (Fig. 4*C* and Fig. S6*B*). Thus, although importin 8 requires the positive patch for binding, its contacts are likely not restricted to this region.

Clinical Relevance of the Importin 8–eIF4E Interaction. Given the nuclear enrichment of eIF4E in M4/M5 AML (Fig. S10), we investigated if importin 8 levels were also dysregulated here (Fig. 5*A*). We observed highly elevated importin 8 protein levels in these AML specimens compared with healthy volunteers. Actin was used as a loading control. These findings suggest that eIF4E might drive its own nuclear accumulation in these AML subtypes (see next section).

The cytoplasmic accumulation of eIF4E upon cap addition (Fig. 4*H*, *Left*) was reminiscent of observations in patients and cell lines treated with ribavirin (9, 14, 15, 23) (Fig. S10). Further, NMR analysis indicated that both the active metabolite of ribavirin, ribavirin 5′-triphosphate (RTP), and m^7G cap binding lead to similar conformational changes to eIF4E and that the phosphates of RTP also bind R157, K159, and K162 (17). Consistently, we observe that RTP also inhibits nuclear import of eIF4E in vitro by over 50-fold, similar to the m^7G cap (Fig. 5*B* and Fig. S1*H*). Thus, similar to the cap, RTP impairs importin 8 binding, preventing nuclear entry of eIF4E, and thereby providing a molecular basis for the cytoplasmic accumulation observed in responding patients.

Importin 8 Is an eIF4E mRNA Export Target. Given the elevated levels of importin 8 in patients with AML who have high eIF4E, we examined whether importin 8 is an eIF4E mRNA export target. First, we carried out immunoprecipitations (IPs) of endogenous eIF4E from the nuclear fraction of U2OS cells and monitored bound RNAs using qPCR. Importin 8 mRNAs were enriched in the eIF4E IPs (Fig. 5*C*). Negative control mRNAs did not immunoprecipitate (e.g., Ubc). We also observed that importin 8 mRNA export and protein levels were elevated upon eIF4E overexpression (Fig. 5 *D* and *E*). Note that 4ESE RNA export elements are found in the 3′ UTRs of target mRNAs (5, 7) and, consistently, modulation of eIF4E did not alter the expression of the importin 8-FLAG construct generated from cDNA in our above foci assays (Fig. S4*A*). Thus, eIF4E elevates importin 8 protein levels through increased mRNA export. Future studies will determine if importin 8 mRNAs are also translation targets of eIF4E.

Discussion

We identified apo-eIF4E, but not eIF4E complexed to cap analogs, RTP, or m^7G-capped RNAs, as an importin 8 cargo (Fig. 5*F*). A positively charged patch on apo-eIF4E at the unoccupied cap-binding site is important for binding importin 8. These observations have significant functional implications. For instance, eIF4E that is associated with actively translating mRNAs is not a cargo. Importin 8 may also sequester eIF4E from target RNAs in the cytoplasm as a means of translational control; this possibility is an important area of future study. Another ramification is that eIF4E–mRNA export complexes would not be reimported into the nucleus until after the cargo release step, reducing futile mRNA export cycles in this way. This cap-dependent switch also provides a molecular explanation for the cytoplasmic accumulation of eIF4E in patients responding to ribavirin and in cell lines treated with ribavirin or cap analogs. Specifically, RTP prevents importin 8 binding to eIF4E, leading to its cytoplasmic retention as observed in patients responding to ribavirin. However, at relapse, when ribavirin is either glucuronidated or not transported into the cell (14, 18), eIF4E is once again an importin 8 cargo and thereby accumulates in the nuclei of leukemic cells. This accumulation leads to elevated eIF4E-dependent mRNA export and is correlated with disease progression. Further, the nuclear accumulation of eIF4E in AML, coupled to its elevated mRNA export activity, suggests that cytoplasmic dwell times must be short for newly exported eIF4E-RNPs relative to the time required to form export-ready eIF4E–mRNA complexes in the nucleus. This possibility is consistent with eIF4E-dependent changes to the nuclear pore complex, which specifically enhance cytoplasmic release of eIF4E-RNA cargoes (6). Finally, our studies suggest a link between the nuclear trafficking of eIF4E and its oncogenic potential.

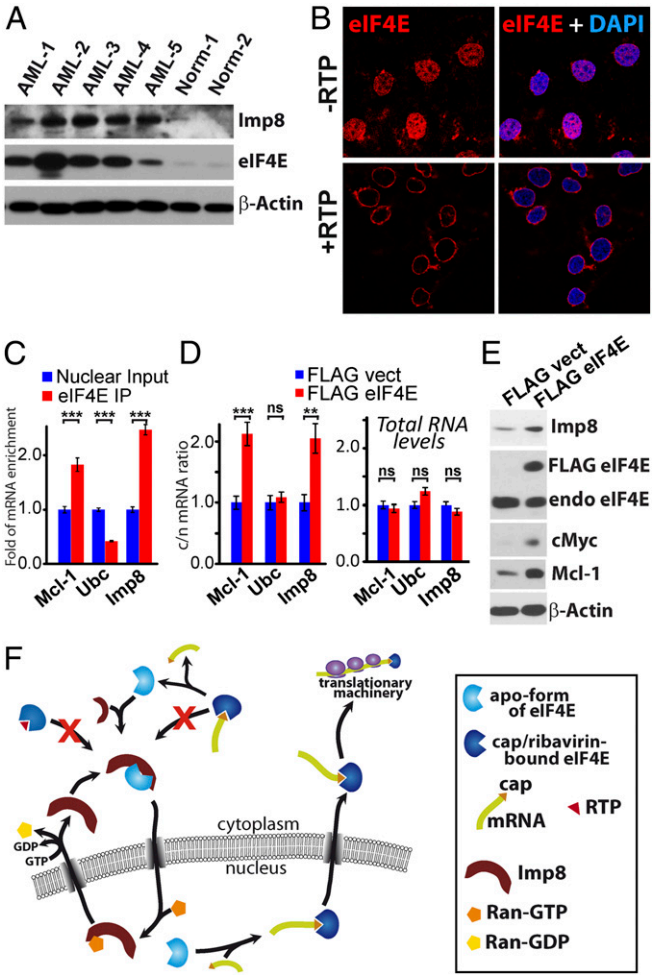

Fig. 5. Importin 8 is elevated in AML and is an eIF4E mRNA export target. (*A*) Importin 8 protein levels in patients with M4/M5 AML by Western blot. Numbers refer to different patients, and normal (Norm) refers to specimens from two different healthy volunteers. Actin is a loading control. (*B*) Nuclear import assays using wild-type eIF4E-GST (red) as a function of treatment with RTP at 50 μM, a clinically achievable concentration (9). DAPI is in blue. Confocal micrographs represent single sections through the plane of the cells with a magnification of 63× and no additional zoom. Quantification is shown in Fig. S1*H*. (*C*) Fold mRNA enrichment relative to nuclear input in eIF4E IPs from U2OS nuclear lysates as indicated. (*D*, *Left*) RNA export assay showing the mRNA *c*/*n* for importin 8 mRNAs. (*D*, *Right*) Total mRNA levels for Ubc, importin 8, and Mcl-1 do not change upon eIF4E overexpression. Data are the mean ± SD. $^{**}P < 0.01$; $^{***}P < 0.001$. ns, not significant. (*E*) Western blot analysis indicates that eIF4E overexpression increases importin 8 levels. (*F*) Model for eIF4E import cycle. Details are provided in the main text.

Aside from eIF4E, Argonaute, SMADs (SMA- and MAD-related proteins), and SRP19 (signal recognition peptide 19) have been reported as importin 8 cargoes (32–34). Unfortunately, no common features emerged after sequence analysis of these cargoes; however, our results suggest there is a strong electrostatic component. This possibility is consistent with our previous observation that the NLS for Kap108 (yeast importin 8) cargoes maps to disordered basic regions (35–38), although our findings here suggest that these surfaces can also be within folded domains. The principles for molecular recognition will likely become more evident once importin 8 cargo structures are determined.

Although importin 8 is the only direct mediator of eIF4E nuclear entry identified to date, it is entirely possible that other karyopherins may be found in the future to traffic eIF4E. Potential

binding partners may indirectly modulate eIF4E nuclear localization, such as the hematopoietically expressed proline-rich homeodomain protein (PRH/Hex), which, when overexpressed, leads to cytoplasmic accumulation of eIF4E (39). Indeed, Hex overexpression impairs the transformation potential of eIF4E, which is linked to inhibition of its nuclear entry (39). Hex, which directly binds eIF4E, may compete with importin 8 for eIF4E, providing a molecular basis for the observed cytoplasmic phenotype. It is likely that other direct binding partners also play roles in eIF4E trafficking, particularly any that modulate cap binding or associate with the positive patch recognized by importin 8. In this way, concentrations and affinities of eIF4E partners will have an impact on importin 8 binding and subsequent eIF4E nuclear trafficking. Thus, it is important to note when considering our findings that importin 8 transcripts themselves are nuclear export targets of eIF4E. However, eIF4E does not abnormally accumulate in the nuclei of all high-eIF4E cancer cells. In this way, nuclear import of eIF4E is likely regulated in a multifactorial and context-dependent manner. In conclusion, these studies provide a molecular basis for nuclear import of eIF4E and an understanding of how ligand binding modulates this process in cells and patients.

Materials and Methods

The eIF4E (pET-15b or pGEX-6p1) and importin 8 (pGEX-4T3) were purified from BL21(DE3) cells. Karyopherin binding assays were conducted in 20 mM Hepes (pH 7.4), 110 mM potassium acetate, 2 mM magnesium acetate, 0.005% Nonidet P-40, 1 mM EGTA, and 20 mM DTT. NMR spectra were acquired at 600 MHz on a Varian INOVA or Bruker Avance III HD spectrometer at 20 °C. Data were processed and analyzed with NMRPipe (40) and Sparky (41) software. PyMOL (42) and Chimera (43) were used for structure rendering. The calculation and analyses of the electrostatic potentials were performed using PDB2PQR (44) and APBS (45). Standard methods for cell culture and transfections were used, as described by Culjkovic et al. (5). The fractionation protocol was followed as described (3, 6). For anchorage-dependent foci assays, 500 cells were seeded per 10-cm plate for 14 d (6) and then stained with Giemsa (Sigma). For nuclear import assays, we used in vitro nuclear import assays as described by Cassany and Gerace (27). Further information is provided in *SI Materials and Methods*.

For all patients in this study, written informed consent was obtained in accordance with the Declaration of Helsinki. This study received institutional review board (all sites) and Health Canada approval.

ACKNOWLEDGMENTS. We thank Garen Collett for initial experiments that detected importin 8 binding to eIF4E, Sanamerjit Mann for technical assistance, and Hualin Zhong for the GST-NLS-GFP construct. We are grateful for specimens from the Banques de Cellules Leucémiques Du Québec. This research was supported by NIH Grants R01 98571 and R01 80728; Translational Research Program grants from the Leukemia and Lymphoma Society (to K.L.B.B.); NIH Grants R01 GM069909 (to Y.M.C.) and U01 GM98526 (to Y.M.C.); the University of Texas Southwestern Endowed Scholars Program (Y.M.C.); Welch Foundation Grant I-1532 (to Y.M.C.); and a Leukemia and Lymphoma Society Scholar Award (to Y.M.C.). K.L.B.B. holds a Canada Research Chair.

1. Carroll M, Borden KL (2013) The oncogene eIF4E: Using biochemical insights to target cancer. *J Interferon Cytokine Res* 33(5):227–238.
2. Ruggero D, et al. (2004) The translation factor eIF-4E promotes tumor formation and cooperates with c-Myc in lymphomagenesis. *Nat Med* 10(5):484–486.
3. Rousseau D, Kaspar R, Rosenwald I, Gehrke L, Sonenberg N (1996) Translation initiation of ornithine decarboxylase and nucleocytoplasmic transport of cyclin D1 mRNA are increased in cells overexpressing eukaryotic initiation factor 4E. *Proc Natl Acad Sci USA* 93(3):1065–1070.
4. Lejbkowicz F, et al. (1992) A fraction of the mRNA 5′ cap-binding protein, eukaryotic initiation factor 4E, localizes to the nucleus. *Proc Natl Acad Sci USA* 89(20):9612–9616.
5. Culjkovic B, Topisirovic I, Skrabanek L, Ruiz-Gutierrez M, Borden KL (2006) eIF4E is a central node of an RNA regulon that governs cellular proliferation. *J Cell Biol* 175(3):415–426.
6. Culjkovic-Kraljacic B, Baguet A, Volpon L, Amri A, Borden KL (2012) The oncogene eIF4E reprograms the nuclear pore complex to promote mRNA export and oncogenic transformation. *Cell Reports* 2(2):207–215.
7. Culjkovic B, Topisirovic I, Skrabanek L, Ruiz-Gutierrez M, Borden KL (2005) eIF4E promotes nuclear export of cyclin D1 mRNAs via an element in the 3′UTR. *J Cell Biol* 169(2):245–256.
8. Culjkovic-Kraljacic B, et al. (2016) Combinatorial targeting of nuclear export and translation of RNA inhibits aggressive B-cell lymphomas. *Blood* 127(7):858–868.
9. Assouline S, et al. (2009) Molecular targeting of the oncogene eIF4E in acute myeloid leukemia (AML): A proof-of-principle clinical trial with ribavirin. *Blood* 114(2):257–260.
10. Topisirovic I, et al. (2003) Aberrant eukaryotic translation initiation factor 4E-dependent mRNA transport impedes hematopoietic differentiation and contributes to leukemogenesis. *Mol Cell Biol* 23(24):8992–9002.
11. Deschler B, de Witte T, Mertelsmann R, Lübbert M (2006) Treatment decision-making for older patients with high-risk myelodysplastic syndrome or acute myeloid leukemia: Problems and approaches. *Haematologica* 91(11):1513–1522.
12. Deschler B, Lübbert M (2006) Acute myeloid leukemia: Epidemiology and etiology. *Cancer* 107(9):2099–2107.
13. Pulsoni A, et al. (2004) Survival of elderly patients with acute myeloid leukemia. *Haematologica* 89(3):296–302.
14. Assouline S, et al. (2015) A phase I trial of ribavirin and low-dose cytarabine for the treatment of relapsed and refractory acute myeloid leukemia with elevated eIF4E. *Haematologica* 100(1):e7–e9.
15. Kentsis A, Topisirovic I, Culjkovic B, Shao L, Borden KL (2004) Ribavirin suppresses eIF4E-mediated oncogenic transformation by physical mimicry of the 7-methyl guanosine mRNA cap. *Proc Natl Acad Sci USA* 101(52):18105–18110.
16. Kentsis A, et al. (2005) Further evidence that ribavirin interacts with eIF4E. *RNA* 11(12):1762–1766.
17. Volpon L, Osborne MJ, Zahreddine H, Romeo AA, Borden KL (2013) Conformational changes induced in the eukaryotic translation initiation factor eIF4E by a clinically relevant inhibitor, ribavirin triphosphate. *Biochem Biophys Res Commun* 434(3):614–619.
18. Zahreddine HA, et al. (2014) The sonic hedgehog factor GLI1 imparts drug resistance through inducible glucuronidation. *Nature* 511(7507):90–93.
19. Bollmann F, et al. (2013) Human inducible nitric oxide synthase (iNOS) expression depends on chromosome region maintenance 1 (CRM1)- and eukaryotic translation initiation factor 4E (eIF4E)-mediated nucleocytoplasmic mRNA transport. *Nitric Oxide* 30:49–59.
20. Pettersson F, et al. (2015) Genetic and pharmacologic inhibition of eIF4E reduces breast cancer cell migration, invasion, and metastasis. *Cancer Res* 75(6):1102–1112.
21. Pettersson F, et al. (2011) Ribavirin treatment effects on breast cancers overexpressing eIF4E, a biomarker with prognostic specificity for luminal B-type breast cancer. *Clin Cancer Res* 17(9):2874–2884.
22. Dostie J, Lejbkowicz F, Sonenberg N (2000) Nuclear eukaryotic initiation factor 4E (eIF4E) colocalizes with splicing factors in speckles. *J Cell Biol* 148(2):239–247.
23. Cohen N, et al. (2001) PML RING suppresses oncogenic transformation by reducing the affinity of eIF4E for mRNA. *EMBO J* 20(16):4547–4559.
24. Chook YM, Süel KE (2011) Nuclear import by karyopherin-βs: Recognition and inhibition. *Biochim Biophys Acta* 1813(9):1593–1606.
25. Chook YM, Blobel G (1999) Structure of the nuclear transport complex karyopherin-beta2-Ran x GppNHp. *Nature* 399(6733):230–237.
26. Wente SR, Rout MP (2010) The nuclear pore complex and nuclear transport. *Cold Spring Harb Perspect Biol* 2(10):a000562.
27. Cassany A, Gerace L (2009) Reconstitution of nuclear import in permeabilized cells. *Methods Mol Biol* 464:181–205.
28. Osborne MJ, et al. (2013) eIF4E3 acts as a tumor suppressor by utilizing an atypical mode of methyl-7-guanosine cap recognition. *Proc Natl Acad Sci USA* 110(10):3877–3882.
29. Topisirovic I, et al. (2009) Molecular dissection of the eukaryotic initiation factor 4E (eIF4E) export-competent RNP. *EMBO J* 28(8):1087–1098.
30. Volpon L, Osborne MJ, Topisirovic I, Siddiqui N, Borden KL (2006) Cap-free structure of eIF4E suggests a basis for conformational regulation by its ligands. *EMBO J* 25(21):5138–5149.
31. Rosorius O, et al. (1999) Direct observation of nucleocytoplasmic transport by microinjection of GFP-tagged proteins in living cells. *Biotechniques* 27(2):350–355.
32. Dean KA, von Ahsen O, Görlich D, Fried HM (2001) Signal recognition particle protein 19 is imported into the nucleus by importin 8 (RanBP8) and transportin. *J Cell Sci* 114(Pt 19):3479–3485.
33. Weinmann L, et al. (2009) Importin 8 is a gene silencing factor that targets argonaute proteins to distinct mRNAs. *Cell* 136(3):496–507.
34. Yao X, Chen X, Cottonham C, Xu L (2008) Preferential utilization of Imp7/8 in nuclear import of Smads. *J Biol Chem* 283(33):22867–22874.
35. Cansizoglu AE, Lee BJ, Zhang ZC, Fontoura BM, Chook YM (2007) Structure-based design of a pathway-specific nuclear import inhibitor. *Nat Struct Mol Biol* 14(5):452–454.
36. Cingolani G, Petosa C, Weis K, Müller CW (1999) Structure of importin-beta bound to the IBB domain of importin-alpha. *Nature* 399(6733):221–229.
37. Kobayashi J, Matsuura Y (2013) Structural basis for cell-cycle-dependent nuclear import mediated by the karyopherin Kap121p. *J Mol Biol* 425(11):1852–1868.
38. Lee BJ, et al. (2006) Rules for nuclear localization sequence recognition by karyopherin beta 2. *Cell* 126(3):543–558.
39. Topisirovic I, et al. (2003) The proline-rich homeodomain protein, PRH, is a tissue-specific inhibitor of eIF4E-dependent cyclin D1 mRNA transport and growth. *EMBO J* 22(3):689–703.
40. Delaglio F, et al. (1995) NMRPipe: A multidimensional spectral processing system based on UNIX pipes. *J Biomol NMR* 6(3):277–293.
41. Goddard TD, Kneller DG (2003) Sparky 3 (University of California, San Francisco).
42. Schrödinger LLC (2014) The PyMOL Molecular Graphics System (Schrödinger, LLC), Version 1.7.4.
43. Pettersen EF, et al. (2004) UCSF Chimera–a visualization system for exploratory research and analysis. *J Comput Chem* 25(13):1605–1612.
44. Dolinsky TJ, Nielsen JE, McCammon JA, Baker NA (2004) PDB2PQR: An automated pipeline for the setup of Poisson-Boltzmann electrostatics calculations. *Nucleic Acids Res* 32(Web Server issue):W665–W667.
45. Baker NA, Sept D, Joseph S, Holst MJ, McCammon JA (2001) Electrostatics of nanosystems: application to microtubules and the ribosome. *Proc Natl Acad Sci USA* 98(18):10037–10041.
46. Culjkovic B, et al. (2008) The eIF4E RNA regulon promotes the Akt signaling pathway. *J Cell Biol* 181(1):51–63.